



Published in final edited form as:

*Annu Rev Anal Chem (Palo Alto Calif)*. 2020 June 12; 13(1): 45–65. doi:10.1146/annurev-anchem-091619-102649.

## 3D Printed Microfluidics

Anna V. Nielsen<sup>†</sup>, Michael J. Beauchamp<sup>†</sup>, Gregory P. Nordin<sup>‡</sup>, Adam T. Woolley<sup>†,\*</sup>

<sup>†</sup>Department of Chemistry and Biochemistry, Brigham Young University, Provo, UT 84602, USA

<sup>‡</sup>Department of Electrical and Computer Engineering, Brigham Young University, Provo, UT 84602, USA

### Abstract

Traditional microfabrication techniques suffer from several disadvantages including inability to create truly three-dimensional architectures, expensive and time-consuming processes when changing device designs, and difficulty in transitioning from prototyping fabrication to bulk manufacturing. 3D printing is an emerging technique that could overcome these disadvantages. While most 3D printed fluidic devices and features to date have been on the millifluidic size-scale, some truly microfluidic devices have been shown. Currently, stereolithography is the most promising approach for routine creation of microfluidic structures, but several approaches under development also have potential. Microfluidic 3D printing is still in a budding stage, similar to where PDMS was two decades ago. With additional work to advance printer hardware and software control, expand and improve resin and printing material selections, and realize additional applications for 3D printed devices, we foresee 3D printing as becoming the dominant microfluidic fabrication method.

### Keywords

additive manufacturing; microdevice fabrication; stereolithography; fused-deposition modeling; PolyJet; PDMS

## 1. Introduction

Microfluidics are an important tool for analytical chemistry, offering advantages in reagent consumption, waste generation, process integration, and cost, to name a few. Current methods to produce microfluidic devices involve micromachining, micromilling, hot embossing, and injection molding; however, these processes can be time consuming, imprecise, expensive, or challenging for design changes. In addition, they often require a dust free (cleanroom) environment to ensure error free devices. Microfluidic devices made by conventional means also lack a truly three-dimensional architecture and flexibility in device design. Lastly, the materials commonly used to fabricate microfluidic devices have drawbacks such as surface adsorption and solvent swelling for polydimethylsiloxane (PDMS), or gas impermeability and rigidity of thermoplastics such as polymethyl methacrylate (PMMA) or cyclic olefin copolymer (COC). While microfluidics are an

\*Corresponding Author: atw@byu.edu.

important and promising tool to perform many analyses, the fabrication of these devices is still less than ideal. A better fabrication method is needed that will allow for cheaper, easier, and faster iterative prototyping and manufacturing of microfluidic devices in many different materials.

One technique that has recently gained traction for fabricating microdevices is 3D printing, which offers several advantages over traditional fabrication techniques. Designs for 3D prints are easily edited and reprinted, thus allowing for testing-based optimization. Additionally, 3D printed devices do not require a cleanroom fabrication environment. The consumables for 3D printing are often only the resin and solvent to remove support materials, so costs can be low. Finally, 3D printing can fully utilize all three dimensions in device architecture, which should allow unique capabilities to be realized.

There are many published reviews that give excellent overviews of 3D printing to define terminology and give basic process overviews (1-12). These articles give good introductions to the field, and we will not belabor those points here. Instead, this work will focus on recent advances in 3D of printing microfluidic devices, as well as opportunities for future directions of research.

## 2. Millifluidics

One of the most well-developed areas of 3D printing for chemical and biological analyses is termed “millifluidics” (13). Large microfluidic to millifluidic devices consist of 3D printed fluidic features  $>200\ \mu\text{m}$ , fabricated using stereolithography (SLA), PolyJet (PJ), or fused deposition modeling (FDM) 3D printers. For many 3D printers, particularly for PJ and FDM, millifluidic features are the smallest that the printer is capable of producing. Though many manufacturers advertise  $<100\ \mu\text{m}$  resolution, deliverable fluidic feature size is typically many times larger than that. This is particularly true for internal features, which are significantly more difficult to create than surface structures. Although there are many applications that can only be realized in the microfluidic size domain, millifluidic devices open up some applications and have been the subject of many publications. Devices built this way can consist of either passive or actively controlled features.

### 2.1 Passive Millifluidic Features

Passive millifluidics include features such as channels, reservoirs, and fluid control structures (14) that are not connected to an external input to activate the device. One example is coiled channels created by Lazarus’ group (15), which were filled with electrically driven, magnetic, or conductive fluids to create electronic mimics such as inductors, transformers, and wireless power coils. Another example is the laminar flow controlled devices developed by Loessberg-Zahl et al. (16), which were used to inject dye into gel as a mimic for targeted drug delivery. Optofluidic microviscometers were fabricated using 3D printing methods and applied to assess the degree of adulteration in milk (17) or the viscosity of blood (18).

Another type of commonly printed feature in devices with passive channels is a fluidic mixer. These mixers typically consist of channels configured to cause multiple fluid streams

from independent inputs to mix. Numerous examples of these 3D printed devices have been published (19-25) including ones from the groups of Breadmore (26), Folch (27), and Malmstadt (28) (Figures 1A, B, and C, respectively). While an important aspect of these mixers is that they can be used in a variety of applications, a downside is the size of the features; with  $>200\ \mu\text{m}$  channels, significant dead volume is present and many stages are needed to fully mix solutions.

Fluid mixers, along with many other passive features, are often dependent on the device material's surface properties; a comprehensive characterization of the surface roughness, transparency, and sealing to glass or other materials can be important considerations (29). However, due to the nature of 3D printing, attention must also be paid to the type of printer being used to create the device, as this can play a significant role in surface properties and feature size (30-31). Additionally, printer settings such as the angle and orientation of material deposition during printing can also affect, and sometimes be leveraged (32) for, specific surface properties. Usually, SLA 3D printers yield the smoothest surfaces and the best resolution (33), however, many applications can still be realized using rougher, millifluidic-sized features.

## 2.2 Active Millifluidic Features

In contrast to passive fluidic features, active ones require connections to an external input to activate. A commonly created active feature is a valve, and by extension, a pump. Though 3D printed valves can have several different configurations, one of the common types uses a deflected membrane to seal parts of channels to drive fluid flow, such as those from the groups of Thiele (34), Folch (35), and Nordin (36). Though this type of valve is commonly produced with PDMS, doing so with a 3D printer often requires extra consideration regarding the flexibility and strength of the printed material. Since this can be difficult, other types of valves can sometimes be preferable. For example, Ismagilov et al. (37) created an alternate pump design which was powered by an evaporating liquid vapor pressure system, and Wu's group (38) created a rotating valve that used manually applied torque to drive fluid flow. While valves are a useful and important component of many fluidic analyzers, they are active components and often require connections to external pressure or pumps to deliver fluid. Additionally, with commercial 3D printer and material capabilities, most valves created are quite large (some  $>1\ \text{mm}$ ), leading to substantial dead volume (smaller valves are discussed in Section 4).

Another active device component which has gained considerable interest is a droplet generator, and several groups have worked to create such 3D printed features and assess their performance. Similar to many other fluidic features, the performance of a droplet generator can be quantitated, both by analyzing the size of the droplets (39) and by comparing droplet homogeneity in a 3D printed device to that in established materials such as PDMS (40). In addition to single-layer droplets, 3D printed devices have also been used to create multilayer droplets (41-42) (i.e., oil/water/oil or water/oil/water) like those shown in Figure 1D. Notably, with 3D printed devices, droplet production can easily be scaled up by using many parallel generators that feed into a single collection zone (43).

Once created, a droplet generator can be placed within the larger framework of a complete analytical device via integration with other components. For example, Morgan et al. (44) combined a generator module with T-junctions and flow focusing chambers to encapsulate stem cells, while Roux's lab (45) produced a special adapter with a series of conical nozzles that could be connected to three different fluidic inputs to create nutrient-enriched spheroids to grow neuronal cells. As cell-based assays are among the most common applications of droplet microfluidics, these are both interesting and important applications of 3D printed devices. However, in both cases, the channel sizes are large (most droplet generator channels are  $>500\ \mu\text{m}$ ), which does not allow applications where smaller droplets are needed, such as for single-cell manipulation.

### 2.3 Integrated Millifluidic Devices

As with conventionally fabricated microfluidics, 3D-printed fluidic devices become more useful for analyses when some amount of integration is achieved. Such integration could involve the incorporation of external components such as optical fibers for spectroscopic analysis (31, 46-47), electrodes for electrochemiluminescence detection (48-50) or stripping voltammetry (51), or packed beads(52-53) or sorbent beds (54) for chromatographic analysis. Alternatively, such integration could involve the joining of several on-chip components or sample pre-processing steps (49) such as the previously mentioned droplet generators (44-45) or like Sochol and coworkers (55) performed with their fluidic circuitry. In some instances, the integration of features is made possible simply by the multi-material nature of 3D printing, such as a printed membrane for reagent diffusion (56).

While the previously cited examples primarily dealt with the creation of 3D printed structures for spectroscopic, chromatographic, or electrochemical assays, there also has been significant interest in developing cellular analyses. For cells, material biocompatibility is a major concern. In an effort to obtain more widely applicable devices, Folch's lab has developed a resin and method for treating poly(ethylene glycol) diacrylate (PEGDA) millifluidic devices to render finished devices biocompatible (57). Several other groups including those of Wagner (58) and Verpoorte (59) have also tested the biocompatibility of other 3D printing materials for cell-based applications. Several different types of cell-based assays have been performed such as cell sorting using helical-shaped channels (60) and bacterial cell counting in droplets using capacitively coupled contactless conductivity monitoring (61). Another device created by Velasquez-Garcia's lab (62) focused on capturing specific cells and maintaining tumor fragments and cells in fluidic channels in a biocompatible and clear resin. The Spence and Martin labs have been at the forefront of using 3D printed fluidic channels for monitoring cell health and secretion (63-64).

Beyond all of the previously mentioned integrated millifluidic applications, there are a host of other applications that can also be achieved using 3D printed millifluidic devices including DNA gel electrophoresis (65), concentration of biorelevant molecules (66), and assays for parasites like malaria (67). Likely, the full suite of available applications has yet to be realized; however, there are also many improvements that should be made to these millifluidic devices. Researchers are still limited by the resolution of most commercial 3D printers. Many, though not all, of these millifluidic assays were performed on this size scale

because it was the minimum achievable feature size rather than the desired or optimal size. Additional research is needed regarding methods and printing materials that allow for truly microfluidic features to be created.

### 3. Surface and Multi-Material Microfluidics

As more researchers have begun exploring the possibility of using 3D printers to create microfluidic devices, it has become abundantly clear that the advertised specifications of a printer rarely match the minimum printable feature size. This is often because printer resolution measures the mechanical or optical capabilities of the printer (i.e., motor step size, nozzle diameter, pixel size, etc.), even though that resolution may not be possible for printed features. This discrepancy primarily exists because the creation of tiny features is not only dependent upon printer specifications, but also on the print material, the location and shape of the fluidic features being printed, and a host of parameters specific to the printer type (i.e., infill rate, light source power and wavelength, motor speed, etc.).

Because of the difficulties in creating small interior fluidic features, particularly in a material that is a desirable match with the application, many groups have only been able to partially embrace the benefits of 3D printing. Thus, some have settled for using 3D printing in a manner similar to traditional fabrication methods, where only 2D or 2.5D fluidic features are possible. Rather than using 3D printing to perform one-step fabrication of three-dimensional microfluidic devices, many structures are created by either using the print as a template for another material (2D), particularly PDMS, or by bonding printed surfaces together for a pseudo 3D device (2.5D). Although not truly three dimensional, these surface feature devices still allow for rapid device prototyping iterations, but this comes with the complexity of post-print and multi-step processing.

Within these noted constraints, surface feature devices can be advantageous for creating microfluidic structures. Although small interior features can be difficult to fabricate, such high-resolution features, both positive and negative, can be more easily created on a surface than in the interior of a device. The use of surface features also alleviates some material concerns by allowing devices to be constructed from multiple, different, or less-than-ideal materials (i.e., not optically transparent, high surface roughness, etc.). Surface feature devices can be grouped into the following categories: PDMS casts, bonded devices, and embedded features. Each is described below.

#### 3.1 PDMS Casts

PDMS casting or soft lithography was already a common technique for the fabrication of microfluidic devices prior to the introduction of 3D printing to the field. The use of PDMS can be advantageous due to its biocompatibility and ease of use, particularly compared to glass devices. However, this ease of prototyping comes with the inability to bulk manufacture these devices. Indeed, PDMS fabrication requires manual labor to cast, peel, and bond the devices. Nevertheless, PDMS is a common microfluidic device prototyping material, and as such, the 3D printing of molds for making PDMS devices is quickly becoming commonplace.

In casting PDMS on a 3D printed template, it has been observed that the 3D print is not as smooth as the silicon wafers that are often used. As such, the surface roughness of the PDMS after casting must be characterized to see if it is sufficiently smooth to match the application (33, 68), and, depending on the type of printer used to create the template, the surface may be treated with a solvent to smooth these layers (69) (Figure 2A-B).

Likely due to the surface chemistry or roughness of 3D printed templates, several groups have found it necessary to coat the 3D printed template surface prior to PDMS casting (70-71). This coating has the dual purpose of making it easier to peel the PDMS off, as well as providing a barrier to the 3D printed material that may inhibit PDMS polymerization, particularly for SLA templates (which is unfortunate as they are often the smoothest prints) (33). As an alternative to coating the surface for easier liftoff, the 3D printed template can be dissolved away to leave behind the desired structure; however, few groups have used this method effectively. In finding a material that can be easily dissolved without damaging or swelling the PDMS too much, only two-dimensional printing of substrates such as wax (72) or sugar (73) has been shown.

Interestingly, a few methods have been developed by which PDMS soft lithography can take advantage of the full three-dimensional capabilities of 3D printing. While it is not difficult to cast PDMS over a 3D object, as it can easily fill in around the printed template, the difficulty comes from removing the mold. One method to do this is to simply design the piece in such a way that it can be manipulated out of void areas such as by twisting a spiral (68) or pushing the sacrificial material out through the void spaces (74). However, this method is only viable for certain geometries, and no application has yet been shown. Another option was used by Chan et al. (75) by selectively tearing the PDMS during template removal as shown in Figure 2C. The tears were then closed off by the elasticity of the PDMS, and later, more permanently, by additional thermal curing. A final option is to simply dissolve away the 3D printed template after molding is complete (76-77). While this means that each template can only be used once, it also allows embedding of permanent electrical and magnetic components into devices without the need for bonding steps.

### 3.2 Bonded Devices

Rather than only using the 3D printed part as a soft lithography mold, many researchers utilize the 3D print as the device itself (or as part of a device), taking advantage of higher resolution available on the surface, compared to the interior of a device. While this use of surface features to create a device eliminates the need for a master, it still requires some additional processing or bonding time.

Unlike for their molded PDMS counterparts, the bonding procedures for surface features in 3D printed devices are quite numerous. Some chips can be directly printed in the desired substrate to which they will be bonded (78-80), while others are simply sealed with tape (81) or another adhesive. One interesting option is simply to not bond the device at all, but rather to seal both the top and bottom of the channel by sandwiching a structure between two surfaces (Figure 2D) (82-83). More common than either of these approaches, however, is to simply bond two 3D printed pieces together using the same material that the pieces were fabricated from (58). In the case of a photopolymerizable resin, this bonding process can be

as simple as a stamp-and-stick approach followed by UV light exposure. For other plastics, bonding can be performed by chemically softening the material and then pressing the semi-melted pieces together as performed by Anciaux et al. (84) who softened acrylonitrile butadiene styrene (ABS) with acetone vapor.

As mentioned previously, one of the main problems still to be addressed with 3D printed devices is the need for more materials, particularly for SLA and PJ printers that can achieve the smallest features. Especially for applications with a need for a specific reactivity or for optical detection (80), it can be advantageous to embed certain materials into a printed device. One method involves pausing the print at the desired point; placing or gluing the membrane, glass slide, or other insert into place; and then resuming the print (85). However, this method is typically only possible for FDM printers, unless a significant amount of user interaction is involved. Otherwise, it is usually simpler to fabricate a chip in multiple pieces and embed the desired parts during post-print processing (58, 81, 83). Some applications may also require the 3D printed surface to be coated prior to the integration of other components, such as with a sputtered metal coating for an electrical-based assay (86).

#### 4. Improved SLA 3D printing for small channels

One of the most promising areas for 3D printing microfluidic devices involves using digital light processing (DLP) based SLA. As has been demonstrated by several groups, a suite of custom printers and materials has been successfully leveraged to embed microfluidic structures with features routinely  $<50\ \mu\text{m}$ . One of the first demonstrations of custom 3D printing resins looked at the optical penetration of light into a resin and showed the importance of careful matching of optical properties of the resin components to those in the light source (87). The custom resin thus developed was then used to produce microfluidic pumps much smaller than previously demonstrated and close to the sizes needed for microfluidic applications (88). In a further demonstration of the need for custom resin formulations, Thiele's group (34) demonstrated that smaller valves could be printed using a custom resin by mixing photoinitiators and absorbers into a monomer in a higher-resolution commercially available printer. Similarly, Rapp and coworkers (89) demonstrated the need for custom resins by showing how the careful choice of an initiator and absorber allow for multi-wavelength polymerization. These works show that there are critical parameters to optimize 3D printing of microfluidic structures, in terms of careful matching of resins, especially the absorbance of the photoinitiator and absorber, to the light source of the printer in order to effectively control the polymerization of material.

A second emerging area that has allowed for SLA 3D printing of microfluidic devices is the optimization of the printer light source. Malinauskas and coworkers (90) used a femtosecond laser with a translation stage to create high-resolution, large, movable structures that acted as scaffolds for cells and photonic crystals (Figure 3A). Others have also demonstrated novel applications of programmable lasers to reduce the size of microparticle sorting channels (91), or DLP grayscaleing to generate compensation patterns to create  $75\ \mu\text{m}$  channels for multilayer droplet generators (92). Our group built a custom 3D printer to create microfluidic channels with cross sections as small as  $18 \times 20\ \mu\text{m}^2$  in a custom resin formulated for the 385 nm light source in the printer (93). This printer also created a variety

of features to test resolution, including ridges, trenches, and micropillars; optimized resolution facilitated construction of a microfluidic bead trapping device (94), shown in Figure 3B. This printer was further used to construct a wide variety of microfluidic devices for diverse applications such as highly parallel chip-to-chip interconnection for easier interfacing to the macro world (95) (Figure 3C), active mixers (96) (Figure 3D), microchannels for testing immunoaffinity monolith capture and elution of pre-term birth risk biomarkers (97), and a microchip electrophoresis setup for the separation and quantitation of these biomarkers (98).

These works all demonstrate the need for and importance of using appropriately designed materials for 3D printing of microfluidic devices with SLA, and show that current, commercially available printers and resins are insufficient for producing microfluidic feature sizes  $<50\ \mu\text{m}$  that are required for applications such as microchip electrophoresis, single cell analysis, or creating biological structure mimics. At present DLP-SLA is the only 3D printing method that has been able to achieve all the criteria to create truly microfluidic devices.

## 5. Unconventional and New Approaches to 3D Printing

Though FDM, PJ, and SLA are the most common 3D printing methods for creating fluidic structures, other methods are also being evaluated for making microfluidic devices. Many of these new approaches are based, at least partially, on similar technology to the primary three 3D printing methods already described. For example, many printers designed for new materials such as glass (99) or liquid inks (100) are FDM-based and thus deal with those same limitations. However, several emerging strategies have potential to improve the creation of microfluidic devices, as described below.

### 5.1. Liquid-Filled Voids for PJ Printing

One of the main disadvantages to PJ printing of fluidic structures is the clearing of internal voids. These voids must be filled with a sacrificial material which is difficult to clear during post-processing. A recent paper by Castiaux et al. (101), however, may offer an alternative. Rather than using a sacrificial material to fill the voids, this group manually controlled the printer software to allow them to fill the void areas with a glycerol-isopropyl alcohol mixture, and then continued printing on top of the previously printed area. Utilizing this approach along with the appropriate printing orientation, they were able to form channels as small as  $125 \times 54\ \mu\text{m}^2$ . Though this approach requires some manual processing and deeper understanding of the 3D printer and software, it offers a promising route to expanding the possibilities for making sub-100- $\mu\text{m}$  feature PJ microfluidic devices.

### 5.2. Two-Photon Direct Laser Writing (DLW) Polymerization

A common misconception in the fledgling field of 3D printed microfluidics is that the challenges of typical 3D printers only creating millifluidic features can be overcome simply by employing sub-micron-resolution two-photon stereolithography. This option looks attractive initially: two-photon polymerization offers excellent voxel resolution without the need for resins with high UV absorber concentrations. However, the tradeoff for these



features is that DLW is extremely slow and has a very limited printing volume. Microfluidic features are formed one voxel at a time from sets of two photons simultaneously absorbed in the tightly focused laser beam. This need for laser light focused near the diffraction limit is responsible for the high resolution of DLW, but also its very slow build time and small build volume (102).

Because of these severe limitations of DLW, only a few researchers have constructed entire microfluidic devices with these 3D printers (103-105). More typically, individual components that require high resolution can be printed directly into an already-constructed microfluidic device. Some examples of internal features created include membranes (106) or, more innovatively, 3D structures such as bellows transistors (107) and spring coil diodes (108) (Figure 4A) which would be extremely difficult to fabricate using traditional 2D microfabrication methods. When DLW is used to create internal features rather than an entire device, it opens possibilities for novel applications, although scaling to bulk manufacturing remains a concern.

### 5.3. Continuous Liquid Interface Printing (CLIP)

CLIP is a relatively high-speed stereolithographic printing technique that allows for continuous z-axis motion and growth of a print rather than layer-by-layer formation. Originally introduced by Tumbleston et al. (109), such continuous printing is made possible using an oxygen-permeable membrane on the bottom of the resin vat (Figure 4B). When the oxygen mixes with the resin, polymerization is inhibited creating a “dead-zone” that prevents the print from sticking to the vat. The thickness of this dead-zone region is dependent on the build speed (slower speeds yield thicker dead-zones).

Similar to regular SLA printing, feature sizes depend on the resin's light absorbance. However, CLIP resins are further limited in resolution because the printing light must penetrate deep enough into the resin to pass through the dead-zone. Thus, higher printing resolutions are only available at slower printing speeds. Nevertheless, promising work has been done to develop multiple resins for CLIP printers (110-112). Another variation of CLIP has been developed which utilizes two-color irradiation along with a UV inhibitor that coordinates with the UV initiator to create the dead-zone region (113) (Figure 4C). This variation of CLIP allows for thicker, adjustable dead-zone regions by changing the incident light intensities.

Although CLIP has major potential for large-scale manufacturing, it is still a relatively new technology. Several things still need to be evaluated including increasing resolution to achieve microfluidic dimensions and, more importantly, forming enclosed features. As yet the literature has not seen a demonstration of this technology to create a truly microfluidic device.

### 5.4. Computed Axial Lithography (CAL)

A recent paper by Kelly et al. (114) offers a different approach for a rapid SLA-type printing method. They used a series of images from a DLP to expose a polymer resin on a rotating stage (Figure 4D-E). The inspiration for this idea was how 2D slices from a CT scan are used to reconstruct a 3D image (or structure). Using the CAL method, they were able to

construct cm-scale structures in less than one minute. Like SLA, resolution is limited by the viscosity and absorbance of the resin. Some versatility in materials was demonstrated, but this technique has not yet been utilized to make microfluidic devices. Importantly, it has definite potential to enable rapid, scalable 3D print manufacturing.

## 6. Future Directions for 3D Printing

For decades, researchers have believed that microfluidics could revolutionize the way routine diagnostic analyses are performed. However, even with numerous papers published each year, few microfluidic assays ever make it to market. One explanation for the lack of a so-called “killer application” for microfluidics is that although potential killer applications may exist, the available device fabrication techniques, particularly soft lithography, are not scalable to support such applications. Indeed, hundreds of functional designs and devices may never leave a research laboratory because they cannot make the jump from prototype to bulk manufacturing. Notably, 3D printing offers the possibility to fabricate microfluidic devices on both the prototyping and manufacturing scale. However, drawbacks remain (115) that still need to be addressed, such as resolution, commercialization/standardization of enabling technologies, and the development of new approaches.

As discussed above, few 3D printing technologies can reach the small feature size scale that many microfluidic applications require (13). Though some applications can be performed in millifluidic structures, there are many important analyses only possible at the microfluidic size scale, which is not presently achievable with current 3D printers on the market. Additionally, the advertised resolution specifications of a 3D printer rarely equate to achievable feature size, a mismatch attributable both to printer mechanical control and printing material. For FDM, the smallest feature size is often limited by the mechanical reproducibility of filament extrusion, surface striations and roughness, and motor control. For PJ, feature dimensions are constrained by control over droplet spraying and the ability to remove support material. Finally, for SLA, the minimum structure size is often dictated by projected image fidelity (i.e., light focusing and scattering), printing resin absorbance and viscosity, and software control over printing parameters. Thus, solutions to improve resolution are two-fold: better mechanical control over printers via hardware and software, and resin/print material formulations that are specifically designed for 3D printing microfluidics.

Most commercially available printers and resins have been developed for applications that do not require the fine control needed for microfluidics. Typically, publications that demonstrate 3D printed microfluidics involve authors who assume some degree of manual control over printer operation in order to optimize usage. Notably, as both the printer hardware and software become more accommodating, users will be better equipped to access 3D printed microfluidics.

In addition to resins and other materials that improve print resolution, it is important for a broader suite of materials to be developed that allow for more applications. A key limitation in switching to 3D printed devices is that they are unable to retain the same surface modifications or physical properties (i.e., permeability, biocompatibility, etc.) necessary for

their application and which can be achieved in conventionally fabricated devices. Although some work (discussed above) has been done to develop new resins, far more comprehensive efforts will be needed for many applications.

### 6.1 Improvements Specific to FDM and PJ 3D Printing

In addition to the broadly applicable suggested improvements described above, specific technologies could help improve the resolution of FDM and PJ printers to more readily fabricate microfluidic devices. Breadmore's group (30) demonstrated the benefits and drawbacks of various types of 3D printers, indicating the superior resolution and surface roughness of SLA relative to FDM and PJ. One way to improve the feature size is to decrease the size of nozzles in FDM or the size of droplets produced in PJ, since these are primary factors in determining the in-plane resolution of printed devices. This improvement in resolution is likely to improve the surface roughness as well.

A second approach to improve the ability of FDM and PJ to create microfluidic devices is to develop better fabrication materials. Several interesting examples are found in the present literature. Qi's group (116) printed a flexible, stretchable material that also had shape memory and self-healing properties. This material consisted of urethane diacrylate, along with a linear, semicrystalline polymer. Gale's lab (117) produced transparent devices made with FDM strengthened by an annealing process for high temperature and pressure applications such as DNA melting with fluorescence detection. In a comprehensive evaluation of 12 different FDM filaments, Verpoorte and coworkers (59) examined features such as transparency, autofluorescence, biocompatibility, leakage of connections, and the produced channel dimensions. The Spence and Martin groups (101) developed the technique described earlier of liquid filling void spaces in PJ printing to avoid the problem of clearing support material after printing. While each of these works shows resin development leading to interesting applications, only the work of Spence and Martin address the issue of channel size. One difficulty cited in producing channels  $<50\ \mu\text{m}$  is clearing the support material from the channels. Typical commercial support materials are not optimized for removal from microfluidic channels, instead requiring flushing, sonication, and/or heat over many hours. One challenge for the development of custom materials is that their use can void warranties on commercial printers. Additionally, printer manufacturers may not yet see value in developing these resins due to perceived low demand, which is fed by lack of availability in an unfortunate, self-defeating cycle. Improved supports or resins could be removed through mechanisms based on solubility, melting, or viscosity differences between the support and device material. Clearly, novel materials will continue to be critical to improving the resolution of FDM and PJ printers.

### 6.2 Improvements Specific to SLA 3D Printing

One of the most promising venues for producing microfluidic channels  $<50\ \mu\text{m}$  is using custom resins and custom SLA 3D printers. An early paper by Zheng et al. (118) identified several key factors to optimizing SLA 3D printing and introduced parameters such as oxygen content, photon flux and absorber or photoinitiator concentration as potential avenues for tailoring custom resins. Indeed, custom resins from the groups of Thiele (34), Rapp (89), Nordin (87, 93), and Lehtinen (119) have been used to successfully create

smaller channels than was possible with commercial materials. Concurrently, there has been a push for making biocompatible resins using known biocompatible materials like PDMS (120) or similar alternatives such as biologically derived, though highly viscous acrylate resins (121). However, one limitation of many custom high-resolution resins is the color imparted to the printed device from the absorber and photoinitiator. Since most projectors emit visible or long wavelength UV light, most custom printed resins are yellow to orange colored, which can be undesirable for many applications. Deeper UV (~365 nm) light sources in projectors should allow the use of different absorbers whose absorption spectra do not encroach as far into the visible, resulting in devices more favorable to optical detection while maintaining small feature sizes.

In addition to improvements in materials for SLA, there are also great opportunities in the customization of the 3D printers. In a system similar to a two-photon DLW system, Pearre et al. (122) used resonant mirrors to speed up printing but maintain 1  $\mu\text{m}$  resolution. This printer was capable of creating approximately  $400 \times 400 \times 400 \mu\text{m}^3$  cubes in 25 s. In another work focused on optimizing printers, Waldbaur et al. (123) used a DMD-based system that had high resolution (2.5  $\mu\text{m}$  pixels) with a moving stage to address a shortfall of SLA 3D printing, wherein high resolution typically necessitates a small print area. By translating the projected image, large stitched together prints could be created. This issue could also be addressed through parallelism by forming multiple devices in a single print.

Another drawback of SLA printing is its inability to create multimaterial prints; however, Bertana et al. (124) attempted to address this shortcoming by creating a sandwich device having structural features from two commercial resins, to allow PCR on chip. Another type of printer suited to address this multimaterial issue for SLA used an air jet between layers to remove unpolymerized resin from the device surface so any printed layer could contain any amount of different printing resins (125). Ongoing work on optimizing printers could combine aspects such as translation of high-resolution projectors, parallel printing capabilities, and multimaterial SLA printing. An important benefit of these areas of research should also be to help drive the market to make these types of printers and resins commercially available by demonstrating the wide variety of applications that can be addressed through 3D printed SLA microfluidic parts.

### 6.3 New Methods

One of the main disadvantages of the new approaches to 3D printing being developed is that they require additional testing. Several of the methods described in Section 5 such as CLIP and CAL have considerable potential to improve the fabrication of 3D printed microfluidic devices. However, these methods will need to be expanded and the user experience simplified significantly before they can be applied in either prototyping or manufacturing microfluidics. Additionally, more applications, and specifically moving to smaller features, will need to be addressed for these methods to be more broadly adopted.

In addition to those approaches already discussed, there is a need for other new 3D printing methods to be developed. Currently, there are trade-offs that come with each approach, such as resolution vs. build area. Could it be possible to integrate the best parts of each printer type to create a multi-resolution or multi-functional printer that would allow for greater

flexibility and broader application? A disadvantage to this approach, however, is that integration of multiple printing methods or resolutions significantly increases the cost and complexity of the printer. More development is needed to continue lowering the cost of 3D printers while improving the resolution and user flexibility via software control.

## 7. Conclusions

3D printing holds promise to revolutionize microfluidics, not only through faster and cheaper prototyping of devices, but also by providing a pathway to bulk manufacturing and commercialization of applications. Though much progress has recently occurred in relatively few years, there are still many improvements to be made to 3D printing. In many ways, 3D printing of microfluidic devices is at a similar stage to where PDMS and soft lithography were two decades ago. With this perspective, we expect that 3D printing could become the dominant (and best) method for microfluidic device fabrication. However, for this to happen, much more research into material development for all printer types must occur, as well as better dissemination of the important figures of merit for the creation of microfluidic devices (i.e., advertised resolution vs. actual achievable minimum feature size, etc.). Additionally, more applications need to be demonstrated in 3D printed devices. Currently, much of the work being done is simply to characterize a printer's capabilities or compare materials rather than use devices for specific applications. As these applications are more fully realized, commercial 3D printer vendors will be better able to develop and market hardware and software to enable the 3D printing microfluidic revolution.

## Acknowledgements

We thank NIH for funding of this work (R01 EB027096, and R15 GM123405-01A1).

## Sources

1. Dixit CK, Kadimisetty K, Rusling J. 2018 3D-printed miniaturized fluidic tools in chemistry and biology. *Anal. Chem* 10:37–52
2. Layani M, Wang X, Magdassi S. 2018 Novel materials for 3D printing by photopolymerization. *Adv. Mater* 30:1706344
3. Bhattacharjee N, Urrios A, Kang S, Folch A. 2016 The upcoming 3D-printing revolution in microfluidics. *Lab Chip* 16:1720–42 [PubMed: 27101171]
4. Au AK, Huynh W, Horowitz LF, Folch A. 2016 3D-printed microfluidics. *Angew. Chem. Int. Ed* 55:3862–81
5. Waheed S, Cabot JM, Macdonald NP, Lewis T, Guijt RM, et al. 2016 3D printed microfluidic device: enablers and barrier. *Lab Chip* 16:1993–2013 [PubMed: 27146365]
6. Yazdi AA, Popma A, Wong W, Nguyen T, Pan Y, Xu J. 2016 3D printing: an emerging tool for novel microfluidics and lab-on-a-chip applications. *Microfluid. Nanofluid* 20:50
7. Amin R, Knowlton S, Hart A, Yenilmez B, Ghaderinezhad F, et al. 2016 3D-printed microfluidic devices. *Biofabrication* 8:022001 [PubMed: 27321137]
8. Chen C, Mehl BT, Munshi AS, Townsend AD, Spence DM, Martin RS. 2016 3D-printed microfluidic devices: fabrication, advantages and limitations—a mini review. *Anal. Methods* 8:6005–12 [PubMed: 27617038]
9. He Y, Wu Y, Fu J, Gao Q, Qiu J. 2016 Developments of 3D printing microfluidics and applications in chemistry and biology: a review. *Electroanalysis* 28:1658–78
10. Ho CMB, Ng SH, Li KHH, Yoon Y. 2015 3D printed microfluidics for biological applications. *Lab Chip* 15:3627–37 [PubMed: 26237523]

11. Huang Y, Leu MC, Mazumder J, Donmez A. 2015 Additive Manufacturing: current state, future potential, gaps and needs, and recommendations. *J. Manuf. Sci. Eng* 137:014001
12. Gross BC, Erkal JL, Lockwood SY, Chen C, Spence DM. 2014 Evaluation of 3D printing and its potential impact on biotechnology and the chemical sciences. *Anal. Chem* 86:3240–53 [PubMed: 24432804]
13. Beauchamp MJ, Nordin GP, Woolley AT. 2017 Moving from millifluidic to truly microfluidic sub-100- $\mu\text{m}$  cross-section 3D printed devices. *Anal. Bioanal. Chem* 409:4311–19 [PubMed: 28612085]
14. Si Y, Wang T, Li C, Li N, Gao C, et al. 2018 Liquids unidirectional transport on dual-scale arrays. *ACS Nano* 12:9214–22 [PubMed: 29963851]
15. Lazarus N, Bedair SS, Smith GL. 2019 Creating 3D Printed Magnetic Devices with Ferrofluids and Liquid Metals. *Additive Manufacturing* 26:15–21
16. Loessberg-Zahl J, van der Meer AD, van den Berg A, Eijkel JCT. 2019 Flow focusing through gels as a tool to generate 3D concentration profiles in hydrogel-filled microfluidic chips. *Lab Chip* 19:206–13 [PubMed: 30548051]
17. Venkateswaran PS, Sharma A, Dubey S, Aarwal A, Goel S 2016 Rapid and automated measurement of milk adulteration using a 3D printed optofluidic microviscometer (OMV). *IEEE Sensors* 16:3000–07
18. Oh S, Kim B, Lee JK, Choi S. 2018 3D-printed capillary circuits for rapid, low-cost, portable analysis of blood viscosity. *Sens. Actuators B: Chem* 259:103–13
19. Plevniak K, Campbell M, Myers T, Hodges A, He M. 2016 3D printed auto-mixing chip enables rapid smartphone diagnosis of anemia. *Biomicrofluidics* 10:054113 [PubMed: 27733894]
20. Lee JM, Zhang M, Yeong WY. 2016 Characterization and evaluation of 3D printed microfluidic chip for cell processing. *Microfluid. Nanofluid* 20:5
21. Patrick WG, Nielsen AAK, Keating SJ, Levy TJ, Wang CW, et al. 2015 DNA assembly in 3D printed fluidics. *PLOS One* 10:e0143636 [PubMed: 26716448]
22. Lee KG, Park KJ, Seok S, Shin S, Kim DH, et al. 2014 3D printed modules for integrated microfluidic devices. *RSC Adv.* 4:32876–80
23. Borro BC, Bohr A, Bucciarelli S, Boetker JP, Foged C, et al. 2019 Microfluidics-based self-assembly of peptide-loaded microgels: effect of three dimensional (3D) printed micromixer design. *J. Colloid Interface Sci* 538:559–68 [PubMed: 30551068]
24. Tang CK, Vaze A, Rusling JF. 2017 Automated 3D-printed unibody immunoarray for chemiluminescence detection of cancer biomarker proteins. *Lab Chip* 17:484–89 [PubMed: 28067370]
25. Mattio E, Robert-Peillard F, Vassalo L, Branger C, Margailan A, et al. 2018 3D-printed lab-on-valve for fluorescent determination of cadmium and lead in water. *Talanta* 183:201–08 [PubMed: 29567165]
26. Shallan AI, Smejkal P, Corban M, Guijt RM, Breadmore MC. 2014 Cost-effective three-dimensional printing of visibly transparent microchips within minutes. *Anal. Chem* 86:3124–30 [PubMed: 24512498]
27. Kuo AP, Bhattacharjee N, Lee YS, Castro K, Kim YT, Folch A. 2019 High-precision stereolithography of biomicrofluidic devices. *Adv. Mater. Technol* 4:1800395 [PubMed: 32490168]
28. Bhargava KC, Thompson B, Malmstadt N. 2014 Discrete elements for 3D microfluidics. *PNAS.* 111:15013–18 [PubMed: 25246553]
29. Gaal G, Mendes M, de Almeida TP, Piazzetta MHO, Gobbi AL, et al. 2017 Simplified fabrication of integrated microfluidic devices using fused deposition modeling 3D printing. *Sens. Actuators B: Chem* 242:35–40
30. Macdonald NP, Cabot JM, Smejkal P, Guijt RM, Paull B, Breadmore MC. 2017 Comparing microfluidic performance of three-dimensional (3D) printing platforms. *Anal. Chem* 89:3858–66 [PubMed: 28281349]
31. Walczak R, Adamski K. 2015 Inkjet 3D printing of microfluidic structures—on the selection of the printer towards printing your own microfluidic chips. *J. Micromech. Microeng* 25:085013

32. Li F, Macdonald NP, Guijt RM, Breadmore MC. 2017 Using printing orientation for tuning fluidic behavior in microfluidic chips made by fused deposition modeling 3D printing. *Anal. Chem* 89:12805–11 [PubMed: 29048159]
33. Faud NM, Carve M, Kaslin J, Wlodkowic D. 2018 Characterization of 3D-Printed moulds for soft lithography of millifluidic devices. *Micromachines* 9:116
34. Männel MJ, Weigel N, Thiele J. 2019 Multifunctional microfluidic devices from tailored photopolymer formulations. *Proc SPIE 10875. Microfluidics, BioMEMS, and Medical Microsystems XVII*. 1087507
35. Lee YS, Bhattacharjee N, Folch A. 2018 3D-printed quake-style microvalves and micropumps. *Lab Chip* 18:1207–14 [PubMed: 29553156]
36. Rogers CI, Qaderi K, Woolley AT, Nordin GP. 2015 3D printed microfluidic devices with integrated valves. *Biomicrofluidics* 9:016501 [PubMed: 25610517]
37. Begolo S, Zhukov DV, Selck DA, Li L, Ismagilov RF. 2014 The pumping lid: investigating multi-material 3D printing for equipment-free, programmable generation of positive and negative pressures for microfluidic applications. *Lab Chip* 14:4616–28 [PubMed: 25231706]
38. Chan HN, Shu Y, Xiong B, Chen Y, Chen Y, et al. 2016 Simple, cost-effective 3D printed microfluidic components for disposable, point-of-care colorimetric analysis. *ACS Sens.* 1:227–34
39. Duarte LC, Chagas CLS, Ribeiro LEB, Coltro WKT. 2017 3D printing of microfluidic devices with embedded sensing electrodes for generating and measuring the size of microdroplets based on contactless conductivity detection. *Sens. Actuators B: Chem* 251:427–32
40. Donvito L, Galluccio L, Lombardo A, Morabito G, Nicolosi A, Reno M. 2015 Experimental validation of a simple, low-cost, T-junction droplet generator fabricated through 3D printing. *J. Micromech. Microeng* 25:035013
41. Zhang JM, Li EQ, Aguirre-Pablo AA, Thoroddsen ST. 2016 A simple and low-cost fully 3D-printed non-planar emulsion generator. *RSC Adv.* 6:2793–99
42. Ji Q, Zhang JM, Liu Y, Li X, Lv P, et al. 2018 A modular microfluidic device via multimaterial 3D printing for emulsion generation. *Sci. Rep* 8:4791 [PubMed: 29556013]
43. Femmer T, Jans A, Eswein R, Anwar N, Moeller M, et al. 2015 High-throughput generation of emulsions and microgels in parallelized microfluidic drop-makers prepared by rapid prototyping. *ACS Appl. Mater. Interfaces* 7:12635–38 [PubMed: 26040198]
44. Morgan AJL, San Jose LH, Jamieson WD, Wymant JM, Song B, et al. 2015 Simple and versatile 3D printed microfluidics using fused filament fabrication. *PLOS One* 11:e0152023
45. Alessandri K, Feyeux M, Gurchenkov B, Delgado C, Trushko A, et al. 2016 A 3D printed microfluidic device for production of functionalized hydrogel microcapsules for culture and differentiation of human Neuronal Stem Cells (hNSC). *Lab Chip* 16:1593–604 [PubMed: 27025278]
46. Monaghan T, Harding MJ, Harris RA, Friel RJ, Christie SDR. 2016 Customizable 3D printed microfluidics for integrated analysis and optimization. *Lab Chip* 16:3362–73 [PubMed: 27452498]
47. Hampson SM, Rowe W, Christie SDR, Platt M. 2018 3D printed microfluidic device with integrated optical sensing for particle analysis. *Sens. Actuators B: Chem* 256:1030–37
48. Bishop GW, Satterwhite-Warden JE, Bist I, Chen E, Rusling JF. 2016 Electrochemiluminescence at bare and DNA-coated graphite electrodes in 3D-printed fluidic devices. *ACS Sens.* 1:197–202 [PubMed: 27135052]
49. Kadimisetty K, Spak AP, Bhalerao KS, Sharafeldin M, Mosa IM, et al. 2018 Automated 4-sample protein immunoassays using 3D-printed microfluidics. *Anal. Methods* 10:4000–06 [PubMed: 30906426]
50. Santangelo MF, Libertino S, Turner APF, Filippini D, Mak WC. 2018 Integrating printed microfluidics with silicon photomultipliers for miniaturised and highly sensitive ATP bioluminescence detection. *Biosens. Bioelectron* 99:464–70 [PubMed: 28820988]
51. Sun Q, Wang J, Tang M, Huang L, Zhang Z, et al. 2017 A new electrochemical system based on a flow-field shaped solid electrode and 3D-printed thin-layer flow cell: detection of Pb<sup>2+</sup> ions by continuous flow accumulation square-wave anodic stripping voltammetry. *Anal. Chem* 89:5024–29. [PubMed: 28393530]

52. McDonough JR, Law R, Reay DA, Zivkovic V. 2019 Fluidization in small-scale gas-solid 3D-printed fluidized beds. *Chem. Eng. Sci* 200:294–309
53. Eberlin MN, Augusto F, Poppi RJ, Gobbi AL, Hantao LW. 2017 Simple, expendable, 3D-printed microfluidic systems for sample preparation of petroleum. *Anal. Chem* 89:3460–67 [PubMed: 28230979]
54. Calderilla C, Maya F, Cerda V, Leal LO. 2018 3D printed device for the automated preconcentration and determination of chromium (VI). *Talanta* 184:15–22 [PubMed: 29674027]
55. Sochol RD, Sweet E, Glick CC, Venkatesh S, Avetisyan A, et al. 2016 3D printed microfluidic circuitry via multijet-based additive manufacturing. *Lab Chip* 16:668–78. [PubMed: 26725379]
56. Li F, Smejkal P, Macdonald NP, Guijt RM, Breadmore MC. 2017 One-step fabrication of a microfluidic device with an integrated membrane and embedded reagents by multimaterial 3D printing. *Anal. Chem* 89:4701–07 [PubMed: 28322552]
57. Urrios A, Parra-Cabrera C, Bhattacharjee N, Gonzalez-Suarez AM, Rigat-Brugarolas LG, et al. 2016 3D-printing of transparent bio-microfluidic devices in PEG-DA. *Lab Chip* 16:2287–94 [PubMed: 27217203]
58. Takenaga S, Schneider B, Erbay E, Biselli M, Schnitzler Th, et al. 2015 Fabrication of biocompatible lab-on-chip devices for biomedical applications by means of a 3D-printing process. *Phys. Status Solidi A* 212:1347–52
59. Salentijn GIJ, Oomen PE, Grajewski M, Verpoorte E. 2017 Fused deposition modeling 3D printing for (bio)analytical device fabrication: procedures, materials, and applications. *Anal. Chem* 89:7053–61 [PubMed: 28628294]
60. Lee W, Kwon D, Chung B, Yung GY, Au A, Folch A, Jeon S. 2014 Ultrarapid detection of pathogenic bacteria using a 3D immunomagnetic flow assay. *Anal. Chem* 86:6683–88 [PubMed: 24856003]
61. Duartea LC, Figueredo F, Ribeiro LEB, Cortón E, Coltro WKT. 2019 Label-free counting of *Escherichia coli* cells in nanoliter droplets using 3D printed microfluidic devices with integrated contactless conductivity detection. *Anal. Chim. Acta* 1071:36–43 [PubMed: 31128753]
62. Beckwith AL, Borenstein JT, Velasquez-Garcia LF. 2018 Monolithic, 3D-printed microfluidic platform for recapitulation of dynamic tumor microenvironments. *J. Microelectromech. S* 27:1009–22
63. Anderson KB, Lockwood SY, Martin RS, Spence DM. 2013 A 3D printed fluidic device that enables integrated features. *Anal. Chem* 85:5622–26 [PubMed: 23687961]
64. Erkal JL, Selimovic A, Gross BC, Lockwood SY, Walton EL, McNamara S, Martin RS, Spence DM. 2014 3D printed microfluidic devices with integrated versatile and reusable electrodes. *Lab Chip* 14:2023–32 [PubMed: 24763966]
65. Walczak R, Adamski K, Kubicki W. 2018 Inkjet 3D printed chip for capillary gel electrophoresis. *Sens. Actuators B: Chem* 261:474–80
66. Li F, Macdonald NP, Guijt RM, Breadmore MC. 2019 Multimaterial 3D printed fluidic device for measuring pharmaceuticals in biological fluids. *Anal. Chem* 91:1758–63 [PubMed: 30513198]
67. Lim C, Lee Y, Kulinsky L. 2018 Fabrication of a malaria-Ab ELISA bioassay platform with utilization of syringe-based and 3D printed assay automation. *Micromachines* 9:502
68. Hwang Y, Paydar OH, Chandler RN. 2015 3D printed molds for non-planar PDMS microfluidic channels. *Sens. Actuat. A: Phys* 226:137–42
69. Brooks JC, Ford KI, Holder DH, Holtan MD, Easley CJ. 2016 Macro-to-micro interfacing to microfluidic channels using 3D-printed templates: application to time-resolved secretion sampling of endocrine tissue. *Analyst* 141:5714–21 [PubMed: 27486597]
70. Cairone F, Gagliano S, Carbone DC, Recca G, Bucolo M. 2016 Micro optofluidic switch realized by 3D printing technology. *Microfluid. Nanofluid* 20:61
71. Comina G, Suska A, Filippini D. 2014 PDMS lab-on-a-chip fabrication using 3D printed templates. *Lab Chip* 14:424–30 [PubMed: 24281262]
72. Kang K, Oh S, Yi H, Han S, Hwang Y. 2018 Fabrication of truly 3D microfluidic channel using 3D-printed soluble mold. *Biomicrofluidics* 12:014105 [PubMed: 29375726]
73. Qiu J, Gao Q, Zhao H, Fu J, He Y. 2017 Rapid customization of 3D integrated microfluidic chips via modular structure-based design. *ACS Biomater. Sci. Eng* 3:2606–16



74. Stumberger G, Vihar B. 2018 Freeform perfusable microfluidics embedded in hydrogel matrices. *Materials* 11:2529
75. Chan HN, Chen Y, Shu Y, Chen Y, Tian Q, Wu H. 2015 Direct, one-step molding of 3D-printed structures for convenient fabrication of truly 3D PDMS microfluidic chips. *Microfluid. Nanofluid* 19:9–18.
76. Saggiomo V, Velders AH. 2015 Simple 3D printed scaffold-removal method for the fabrication of intricate microfluidic devices. *Adv. Sci* 2:1500125
77. Goh WH, Hashimoto M. 2018 Dual sacrificial molding: fabricating 3D microchannels with overhang and helical features. *Micromachines* 9:523
78. Hamad EM, Bilatto SER, Adly NY, Correa DS, Wolfrum B, et al. 2016 Inkjet printing of UV-curable adhesive and dielectric inks for microfluidic devices. *Lab Chip* 16:70–74 [PubMed: 26627046]
79. Bressan LP, Robles-Najar J, Adamo CB, Quero RF, Costa BMC, et al. 2019 3D-printed microfluidic device for the synthesis of silver and gold nanoparticles. *Microchem. J* 146:1083–89
80. Bressan LP, Adamo CB, Quero RF, de Jesus DP, da Silva JAF. 2019 A simple procedure to produce FDM-based 3D-printed microfluidic devices with an integrated PMMA optical window. *Anal. Methods* 11:1014–20
81. Comina G, Suska A, Filippini D. 2015 3D printed unibody lab-on-a-chip: features survey and check-valves integration dagger. *Micromachines* 6:437–51
82. Kise DP, Reddish MJ, Dyer RB. 2015 Sandwich-format 3D printed microfluidic mixers: a flexible platform for multi-probe analysis. *J. Micromech. Microeng* 25:124002 [PubMed: 26855478]
83. Kadimisetty K, Song J, Doto AM, Hwang Y, Peng J, et al. 2018 Fully 3D printed integrated reactor array for point-of-care molecular diagnostics. *Biosens. Bioelectron* 109:156–63 [PubMed: 29550739]
84. Anciaux SK, Geiger M, Bowser MT. 2016 3D printed micro free-flow electrophoresis device. *Anal. Chem* 88:7675–82 [PubMed: 27377354]
85. Yuen PK. 2016 Embedding objects during 3D printing to add new functionalities. *Biomicrofluidics* 10:044104 [PubMed: 27478528]
86. Marschewski J, Brenner L, Ebejer N, Ruch P, Michel B, Poulidakos D. 2017 3D-printed fluidic networks for high-power-density heat-managing miniaturized redox flow batteries. *Energy Environ. Sci* 10:780–87
87. Gong H, Beauchamp M, Perry S, Woolley AT, Nordin GP. 2015 Optical approach to resin formulation for 3D printed microfluidics. *RSC Adv.* 5:106621 [PubMed: 26744624]
88. Gong H, Woolley AT, Nordin GP. 2016 High density 3D printed microfluidic valves, pumps, and multiplexers. *Lab Chip* 16:2450–58 [PubMed: 27242064]
89. Schmid MC, Wussler D, Kotz F, Rapp BE. 2019 Wavelength-selective negative photoresist for photolithography suitable for generating microstructures with up to three distinct height levels. *Proc SPIE* 10915, *Organic Photonic Materials and Devices XXI*. 1091511
90. Jonusauskas L, Gailevicius D, Rekstyte S, Juodkazis S, Malinauskas M. 2018 Synchronization of linear stages and galvo-scanners for efficient direct laser fabrication of polymeric 3D meso-scale structures. *Proceedings of the SPIE* 10523, *Laser 3D Manufacturing V*. 105230X
91. Juskova P, Ollitrault A, Serra M, Viovy JL, Malaquin L. 2018 Resolution improvement of 3D stereo-lithography through the direct laser trajectory programming: application to microfluidic deterministic lateral displacement device. *Anal. Chim. Acta* 1000:239–47 [PubMed: 29289316]
92. Mannel MJ, Selzer L, Bernhardt R, Thiele J. 2018 Optimizing process parameters in commercial micro-stereolithography for forming emulsions and polymer microparticles in nonplanar microfluidic devices. *Adv. Mater. Technol* 4:1800408
93. Gong H, Bickham BP, Woolley AT, Nordin GP. 2017 Custom 3D printer and resin for 18  $\mu\text{m}$   $\times$  20  $\mu\text{m}$  microfluidic flow channels. *Lab Chip* 17:2899–909 [PubMed: 28726927]
94. Beauchamp MJ, Gong H, Woolley AT, Nordin GP. 2018 3D printed microfluidic features using dose control in X, Y, and Z dimensions. *Micromachines* 9:326
95. Gong H, Woolley AT, Nordin GP. 2018 3D printed high density, reversible, chip-to-chip microfluidic interconnects. *Lab Chip* 18:639–47 [PubMed: 29355276]

96. Gong H, Woolley AT, Nordin GP. 2019 3D printed selectable dilution mixer pumps. *Biomicrofluidics* 13:014106 [PubMed: 30766649]
97. Parker EK, Nielsen AV, Beauchamp MJ, Almughamsi HM, Nielsen JB, et al. 2019 3D printed microfluidic devices with immunoaffinity monoliths for extraction of preterm birth biomarkers. *Anal. Bioanal. Chem* 411:5405–13 [PubMed: 30382326]
98. Beauchamp MJ, Nielsen AV, Gong H, Nordin GP, Woolley AT. 2019 3D printed microfluidic devices for microchip electrophoresis of preterm birth biomarkers. *Anal. Chem* 91:7418–25 [PubMed: 31056901]
99. Gal-Or E, Gershoni Y, Scotti G, Nilsson SME, Saarinen J, et al. 2019 Chemical analysis using 3D printed glass microfluidics. *Anal. Methods* 11:1802–10
100. Chen L, Tang X, Xie P, Xu J, Chen Z, et al. 2018 3D printing of artificial leaf with tunable hierarchical porosity for CO<sub>2</sub> photoreduction. *Chem. Mater* 30:799–806
101. Castiaux AD, Pinger CW, Hayter EA, Bunn ME, Martin RS, Spence DM. 2019 PolyJet 3D-printed enclosed microfluidic channels without photocurable supports. *Anal. Chem* 91:6910–17 [PubMed: 31035747]
102. Bückmann T, Stenger N, Kadic M, Kashke J, Frölich A, et al. 2012 Tailored 3D mechanical metamaterials made by dip-in direct-laser-writing optical lithography. *Adv. Mater* 24:2710–14 [PubMed: 22495906]
103. Mayer F, Richter S, Westhauser J, Blasco E, Barner-Kowollik C, Wegener M. 2019 Multimaterial 3D laser microprinting using an integrated microfluidic system. *Sci. Adv* 5:eaau91
104. di Giacomo R, Krrödel S, Maresca B, Benzoni P, Rusconi R, et al. 2017 Deployable micro-traps to sequester motile bacteria. *Sci. Rep* 2017, 7:45897 [PubMed: 28378786]
105. Son AI, Opfermann JD, McCue C, Ziobro J, Abrahams JH III, et al. 2017 An implantable micro-caged device for direct local delivery of agents. *Sci. Rep* 7:17624 [PubMed: 29247175]
106. Perrucci F, Bertana V, Marasso SL, Scordo G, Ferrero S, et al. 2018 Optimization of a suspended two photon polymerized microfluidic filtration system. *Microelectron. Eng* 195:95–100
107. Alsharhan AT, Acevedo R, Warren R, Sochol RD. 2019 3D microfluidics via cyclic olefin polymer-based in situ direct laser writing. *Lab Chip* 19:2799–810 [PubMed: 31334525]
108. Lamont AC, Alsharhan AT, Sochol RD. 2019 Geometric Determinants of In-Situ Direct Laser Writing. *Sci. Rep* 9:394 [PubMed: 30674934]
109. Tumbleston JR, Shirvanyants D, Ermoshkin N, Januszewicz R, Johnson AR, et al. 2015 Continuous liquid interface production of 3D objects. *Science* 347:1349–52 [PubMed: 25780246]
110. Ware HOT, Farsheed AC, Akar B, Duan C, Chen X, et al. 2018 High-speed on-demand 3D printed bioresorbable vascular scaffolds. *Mater. Chem. Today* 7:25–34
111. Shao G, Ware HOT, Chen X, Li L, Sun C. 2019 High-resolution 3D printing magnetically-active microstructures using micro-CLIP process. *Proc SPIE* 10969. Nano-, Bio-, Info-Tech Sensors and 3D Systems III. 109690M
112. Kuang X, Zhao Z, Chen K, Fang D, Kang G, Qi HJ. 2018 High-speed 3D printing of high-performance thermosetting polymers via two-stage curing. *Macromol. Rapid Commun* 39:1700809
113. de Beer MP, van der Laan HL, Cole MA, Whelan RJ, Burns MA, Scott TF. 2019 Rapid, continuous additive manufacturing by volumetric polymerization inhibition patterning. *Sci. Adv* 5:eaau8723 [PubMed: 30746465]
114. Kelly BE, Bhattacharya I, Heidari H, Shusteff M, Spadaccini CM, Taylor HK. 2019 Volumetric additive manufacturing via tomographic reconstruction. *Science* 363:1075–79 [PubMed: 30705152]
115. Friddin MS, Elani Y, Trantidou T, Ces O. 2019 New directions for artificial cells using rapid prototyped biosystems. *Anal. Chem* 91:4921–28 [PubMed: 30841694]
116. Kuang X, Chen K, Dunn CK, Wu J, Li VCF, Qi HJ. 2018 3D Printing of highly stretchable, shape-memory, and self-healing elastomer toward novel 4D printing. *ACS Appl. Mater. Interfaces* 10:7381–88 [PubMed: 29400445]

117. Romanov V, Samuel R, Chaharland M, Jafek AR, Frost A, Gale BK. 2018 FDM 3D printing of high-pressure, heat-resistant, transparent microfluidic devices. *Anal. Chem* 90:10450–56 [PubMed: 30071717]
118. Zheng X, Deotte J, Alonso MP, Farquar GR, Weisgraber TH, et al. 2012 Design and optimization of a light-emitting diode projection micro-stereolithography three-dimensional manufacturing system. *Rev. Sci. Instrum* 83:125001 [PubMed: 23278017]
119. Lehtinen P, Kaivola M, Korhonen H, Seppälä J, Partanen J. 2017 Producing parts with multiple layer thicknesses by projection stereolithography. *Int. J. Rapid Manuf* 6:087542
120. Bhattacharjee N, Parra-Cabrera C, Kim YT, Kuo AP, Folch A. 2018 Desktop-Stereolithography 3D-Printing of a Poly(dimethylsiloxane)-Based Material with Sylgard-184 Properties. *Adv. Mat* 30:1800001
121. Voet VSD, Strating T, Schnelting GHM, Dijkstra P, Tietema M, et al. 2018 Biobased acrylate photocurable resin formulation for stereolithography 3D printing. *ACS Omega* 3:1403–08 [PubMed: 31458469]
122. Pearre BW, Michas C, Tsang JM, Gardner TJ, Otchy TM. 2018 Fast Micron-Scale 3D Printing with a Resonant-Scanning Two-Photon Microscope. *Appl. Phys arXiv:1803.07135* [physics.app-ph].
123. Waldbaur A, Carneiro B, Hettich P, Wilhelm E, Rapp BE. 2013 Computer-aided microfluidics (CAMF): from digital 3D-CAD models to physical structures within a day. *Microfluid. Nanofluid* 15:625–35
124. Bertana V, Potrich C, Pirri CF, Pedezolli C, Cocuzza M, Marasso SL. 2018 3D-printed microfluidics on thin poly(methyl methacrylate) substrates for genetic applications. *J. Vac. Sci. Technol. B* 36:01A106
125. Kowsari K, Akbari S, Wang D, Fang NX, Ge Q. 2018 High-efficiency high-resolution multimaterial fabrication for digital light processing-based three-dimensional printing. *3D Print. Addit. Manuf* 5:185–93

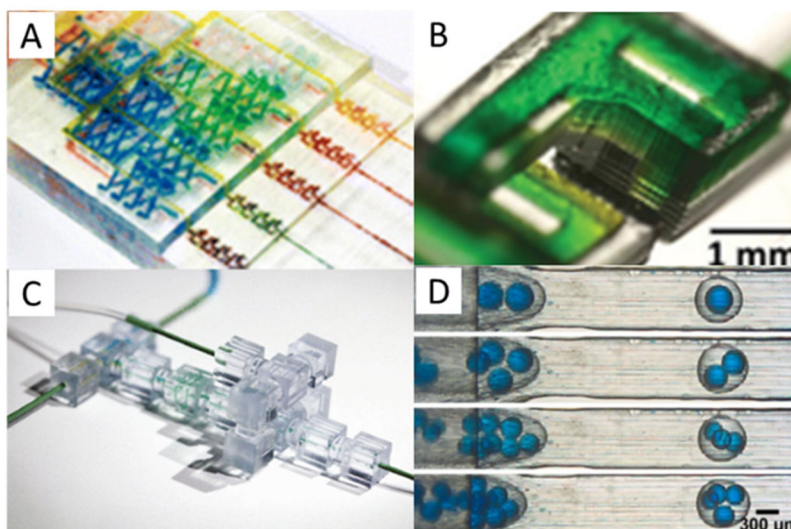


**Figure 1.** Fluidic features produced by 3D printing. A) Gradient mixing device consisting of several intersecting turbulent mixing sections used to measure nitrite concentrations. Reprinted with permission from ref. 26; copyright 2014 American Chemical Society. B) Mixer consisting of several connected “F” shaped units that allow streams of fluid to pass and diffuse into each other. Reprinted with permission from ref. 27. C) 3D printed modular device consisting of several discrete elements produced in cubes which can be connected together to create larger functional devices with several purposes; adapted with permission from ref. 28. D) Droplet generators showing several different water/oil/water droplets containing multiple blue droplets within a single oil droplet; adapted with permission from ref. 42.

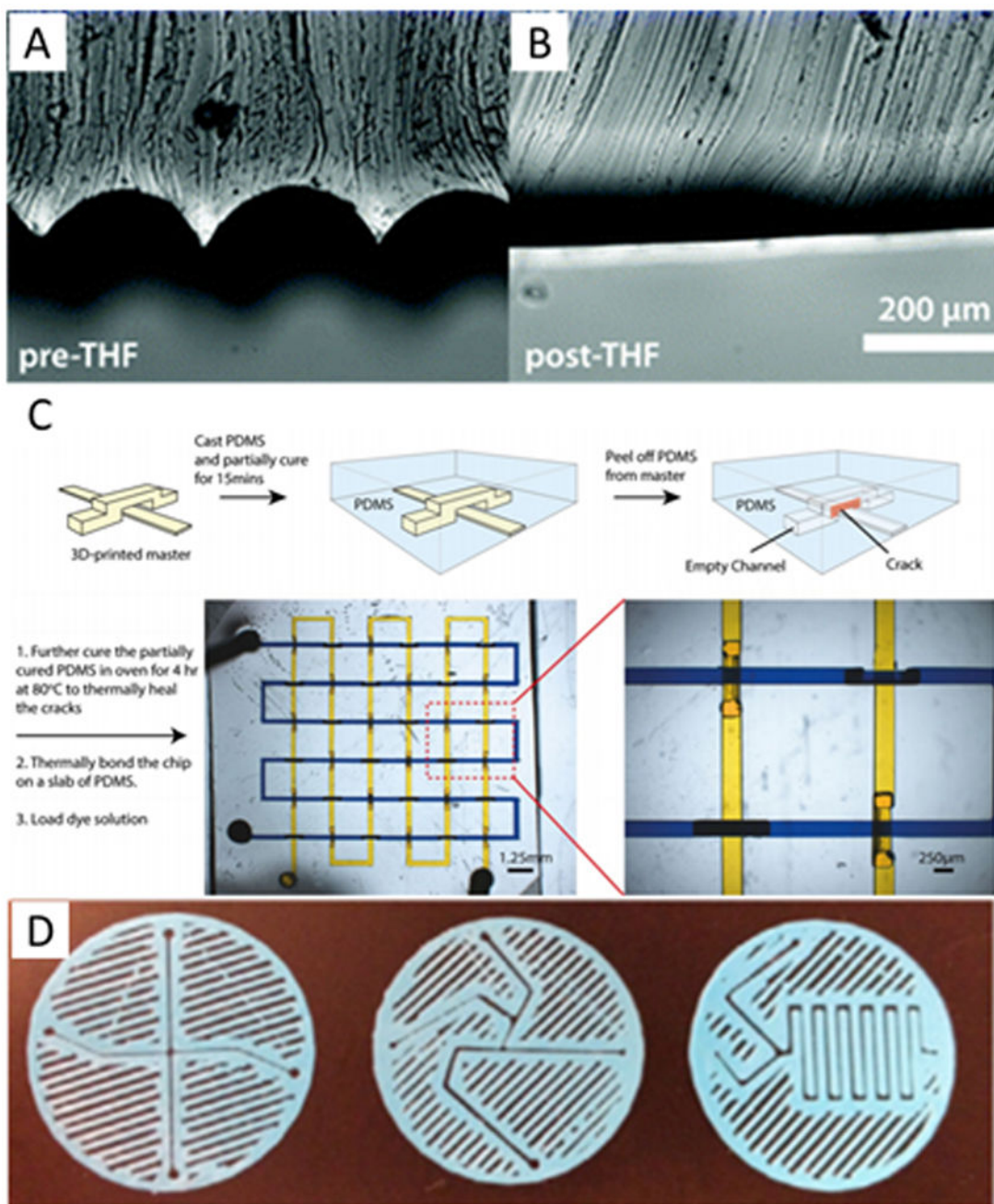


**Figure 2.**

Template and surface 3D printed microfluidic devices. A-B) Images showing the surface roughness of a polylactic acid FDM template before and after smoothing with tetrahydrofuran solvent. Republished with permission of the Royal Society of Chemistry, from ref. 69; permission conveyed through Copyright Clearance Center. C) A method of casting a fully three-dimensional device. PDMS is cast over a 3D printed template and allowed to partially cure. The PDMS is cracked and peeled off the template then allowed to fully cure before filling with fluid for experiments. Reprinted by permission from ref. 75, copyright 2015 Springer Nature. D) Sandwich-style planar mixers printed using FDM then

sandwiched between two surfaces with interface connections to form fluidic devices.  
Republished from ref. 82 with permission of IOP Publishing; permission conveyed through  
Copyright Clearance Center.

Author Manuscript

Author Manuscript

Author Manuscript

Author Manuscript

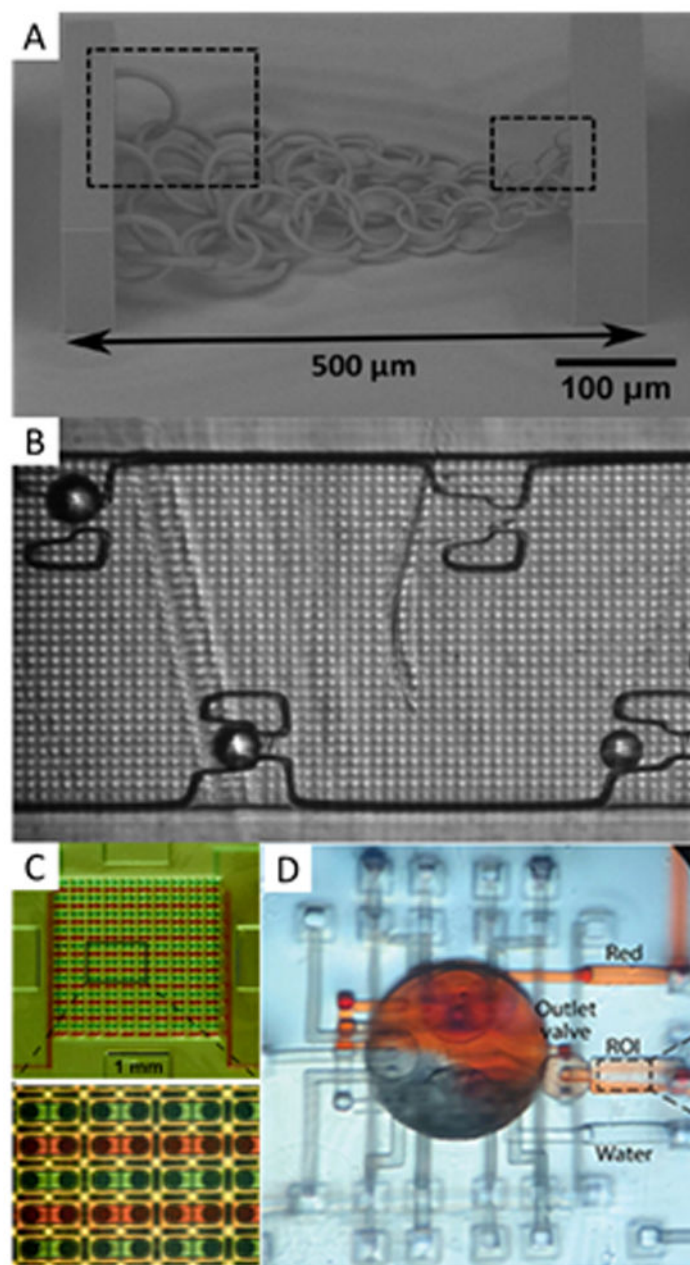


**Figure 3.**

SLA 3D printed microfluidic devices with  $\sim 50 \mu\text{m}$  features. A) Chain-links of varying sizes as small as  $4 \mu\text{m}$ . Reproduced with permission from ref. 90. B) Microfluidic bead trapping device;  $25 \mu\text{m}$  particles were captured in the traps, adapted with permission from ref. 94. C) Interlocking microgaskets used to make a  $20 \times 20$  array of interconnected channels between two discrete devices to facilitate device-to-world interfacing without leaking. Republished from ref. 95 with permission of the Royal Society of Chemistry; permission conveyed through Copyright Clearance Center. D) Mixing device consisting of  $50 \mu\text{m}$  channels with valves and a large mixing chamber in the center. Reprinted from ref. 96, with the permission of AIP Publishing.

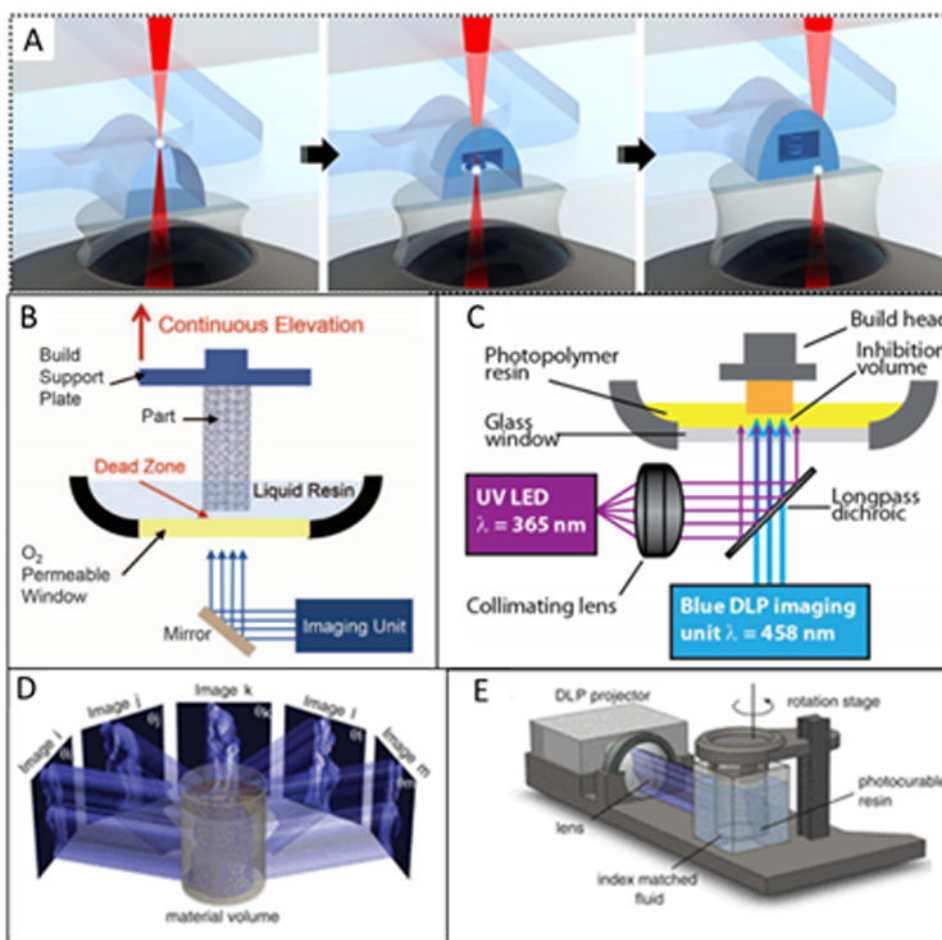


**Figure 4.**

New approaches for 3D printing of microfluidic devices and structures. A) Two-photon polymerization of a spring diode inside a microfluidic channel; adapted with permission from ref. 108. B) Instrumentation setup for CLIP; the build platform is continuously raised out of a resin vat and polymerization is enabled by an oxygen-inhibited “dead zone” above a permeable window. Reprinted from ref. 109 with permission from AAAS. C) Instrumental setup for an alternate approach to CLIP. Polymerization is initiated by the blue light and inhibited by the UV light. Reproduced with permission from ref. 113. D-E) Image angle breakdown and instrumental setup for CAL 3D printing. Reprinted from ref. 114 with permission from AAAS.